On the Statistical Monitoring of Interpersonal Organizational Networks

Marcus B. Perry[1] and Curry W. Hilton[2]
Department of Information Systems, Statistics & Management Science
The University of Alabama
300 Alston Hall
Box 870226
Tuscaloosa, AL 35487

Abstract

Statistical process control (SPC) charts have traditionally been applied to manufacturing processes; however, more recent developments highlight their application to social networks. In this paper, we consider the important problem of detecting changes in an organization's interpersonal networks over time, as shifts in certain graph structural tendencies are interpretable, and can potentially reveal insight into the health of an organization. To this end, we propose an exponentially-weighted moving average (EWMA) control-chart for quickly detecting shifts in the *hierarchical* tendency of directed networks. Although development of the proposed control chart was motivated by network data, our method is generally applicable to multinomial processes. Monte Carlo simulation was used to assess the detection performance of our proposed control chart, relative to that of the multinomial cumulative sum (CUSUM) alternative. Results suggest that if the out-of-control shift in the multinomial probabilities cannot be specified *a priori*, the proposed EWMA control chart should be considered as an alternative to the CUSUM strategy. Application of the proposed method is demonstrated on a real data set; namely, the open source Enron email corpus.

Keywords: Directed networks, hierarchical graph, multinomial process, network monitoring, statistical process control, reciprocity, transitivity.

[1]Dr. Marcus Perry is an Associate Professor of Applied Statistics in the Department of Information Systems, Statistics and Management Science in the Culverhouse College of Commerce at the University of Alabama, Tuscaloosa. His email address is mperry@cba.ua.edu.

[2]Curry W. Hilton is an Applied Statistics PhD student in the Department of Information Systems, Statistics and Management Science in the Culverhouse College of Commerce at the University of Alabama, Tuscaloosa. His email address is curry.hilton@gmail.com.

1 Introduction and Motivation

Statistical process control (SPC) methods have traditionally been applied to industrial processes as a means to monitor the quality of manufactured products. More recently, however, the application of SPC methods to non-manufacturing processes has become more prevalent. In fact, while discussing the "big-data" challenges for SPC practitioners and researchers, Lin (2014) categorizes the types of data to be monitored using SPC methods as follows:

i. Time series 101 - each observation is a scalar

ii. Time series 201 - each observation is a vector

iii. Time series 301 - each observation is a profile

iv. Time series 401 - each observation is a network

v. Time series 501 - each observation is a graphic

The first three data types in the list above are fairly well studied; however, the development and evaluation of methods for monitoring networks and/or graphs is lacking. In this paper, we consider the important problem of detecting changes in an organization's interpersonal networks over time, as shifts in certain graph structural tendencies are interpretable, and can potentially reveal significant insight into the health of an organization.

Although the development and evaluation of SPC methods for network-based systems is in its early stages, the literature does contain some relevant work. Woodall et al. (2017) recently provided a review paper outlining the current state of the literature on SPC methods developed for undirected social network data. Many of the methods cited in their paper considered monitoring for changes in the communication *levels* of a network or subnetwork, while others apply traditional SPC methods to monitor for changes in the average closeness and betweenness of the network. Interpretation of a control chart signal involving the former is often straightforward; however, interpretation of an increase or decrease in the *average* closeness or betweenness of a network is somewhat unclear.

Given the importance of *structural balance* theories in the social network literature, it is surprising that none of the methods discussed in Woodall et al. (2017) considered detecting changes in the structural tendencies of networks. Clearly, an important question about networks concerns whether or not they are highly structured. For example, is there a point in time where interpersonal organizational communications shifted from decentralized to centralized? Such a shift in communication structure might suggest a hierarchical decision-making structure, where all decisions and processes are handled at the top of the organization. An increase

in the hierarchical tendency of an organization's structure could lead to slower decision making, decreased operational efficiency, and less innovation. Further, the *root cause* of such an increase could be associated with conflict or crisis within an organization, e.g., see Danowski and Edison-Swift (1985), Davis et al. (2007), and Diesner et al. (2005), where centralization of functional control is often required during conflict or crisis management.

One means to assessing whether a network is hierarchical is to assess the relationship between its reciprocal and transitive tendencies. Let $c(i, j)$ denote an indicator variable taking the value 1 if communication flows from node i to node j, and zero otherwise. Then, a reciprocal (or mutual) flow between nodes i and j exists if $c(i, j) = c(j, i) = 1$. To describe a transitive flow, let i, j, and k denote three nodes in the network, then there are 6 possible ways to define a transitive flow, as shown in Figure 1. In general, for a network of size n, there are $\binom{n}{2}$ possible reciprocal pairs (or mutual dyads) and $6 \times \binom{n}{3}$ possible transitive triads. For an observed network, the counts of mutual dyads and transitive triads can be easily computed from linear combinations of the triad census of the graph, e.g., see Holland and Leinhardt (1976) and Moody (1998).

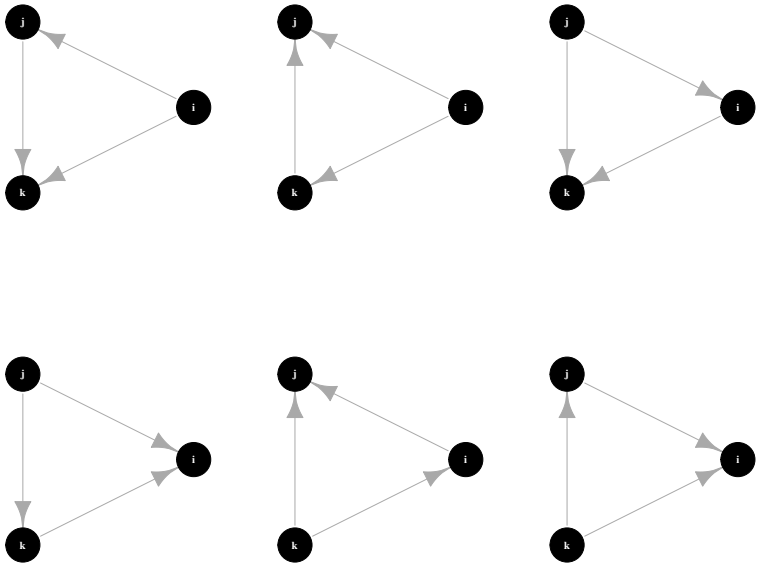

Figure 1: Six possible transitive flows for the triad (i, j, k).

Reciprocity and transitivity of digraphs (or directed graphs) are well studied in the social sciences literature, where the former is linked theoretically to exchange and resource dependence theories, e.g., see Cropanzano and Mitchell (2005) and Hillman et al. (2009), and the latter is linked theoretically to balance theory, originally developed as a theory of cognitive consistency for understanding interper-

sonal structures in a network, e.g., see Heider (1958). While theories of exchange and resource-dependency posit structural tendencies at the dyadic level, theories of cognitive consistency posit structural tendencies at the triadic level.

Holland and Leinhardt (1971) posited that transitivity, as a generalization of balance theory, can lead to the development of hierarchies and cliques, while Contractor et al. (2006) explained that transitive triads in formal relationships within organizational networks point to the presence of hierarchy or centralization. Kilduff and Tsai (2003) suggested that if an organizational network tends towards low reciprocity and high transitivity, this results in a hierarchical flow of communication. This is easy to see if one considers that, in the limit of low reciprocity and high transitivity, one obtains a fully transitive tournament. To construct this type of graph, consider ordering all vertices on the real line, and then placing (i, j) edge in all i, j pairs such that $i > j$. Figure 2 shows a fully transitive tournament with 4 vertices constructed this way. Notice the hierarchical nature of the communication flow for this type of graph. In practice, one does not see anything quite as extreme as the fully transitive tournament, but certainly some networks can tend in such a direction.

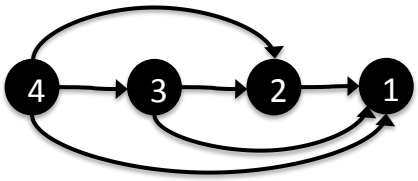

Figure 2: Fully transitive tournament with 4 vertices.

To illustrate further, consider a simple example involving the digraph shown in Figure 3. Suppose this network represents the communication flows expected under normal conditions between faculty members from two different departments within a college. Specifically, let node 1 represent the dean of the college, nodes 2 and 3 represent department heads, and the remaining nodes represent research faculty within their respective departments. Then Figure 3 suggests the expected communication flow between dean and department heads is mutual, and the expected communication flow between faculty members within each department is mutual. Note that the count of reciprocal dyads for this digraph is 14, while the count of transitive triads is 48.

Now, imagine the occurrence of an event that could significantly effect the future of the departments. For example, suppose that budget constraints have resulted in the two departments being considered for merger into a single department, thus creating uncertainly about the future of various academic programs

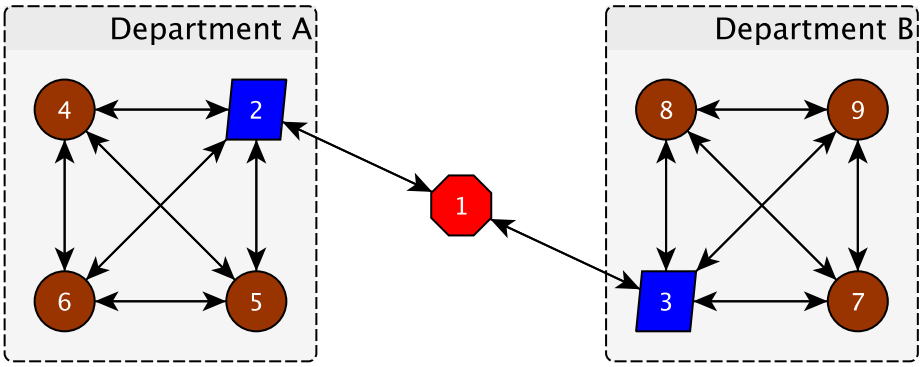

Figure 3: Directed graph for hypothetical example showing expected flows under normal conditions.

and current faculty within the departments. In such a case, one might expect the dean to communicate information relevant to the merger with all faculty directly, i.e., not just through the department heads. Figure 4 shows the communication flows expected as a result of the threat of merger (shown as dashed edges), in addition to the communication flows corresponding to normal operations (shown as solid edges). Notice that, for the network in Figure 4, the number of reciprocal dyads is 14, while the number of transitive triads is 84. Hence, a consequence of the new communication flows assumed to mitigate the effects of the merger is to observe no increase in the mutual dyad count, and a relatively large increase in the transitive triad count. More specifically, as a result of the talk of a merger, an increase in the hierarchical tendency of the communication flows is observed.

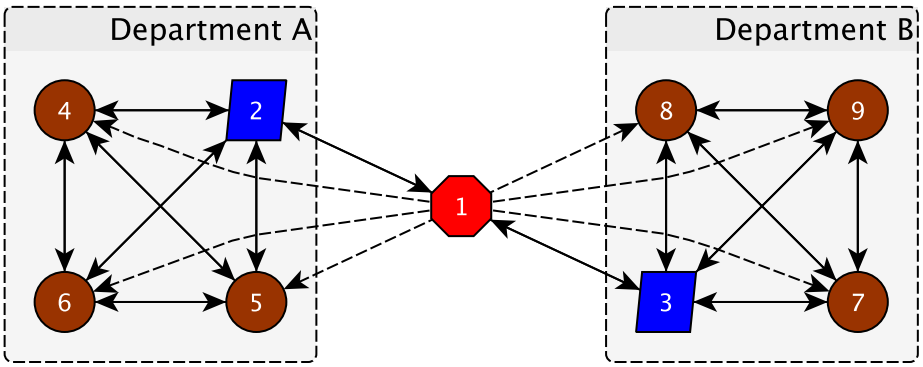

Figure 4: Directed graph for hypothetical example showing expected flows under normal conditions plus flows resulting from threat of merger.

From this simple illustration, one can imagine how an increase in the hierarchical tendency of an organization's communications network could be indicative of an organization that is undergoing some level of conflict or crisis. However, that's not the only interpretation. Suppose that instead of a network of college faculty communications, the network above represented the communication flows of a terrorist or criminal organization. Then an increase in the hierarchical tendencies of such a network might suggest the possibility of planned criminal activity in the near future, i.e., drug trafficking, terrorist attack, etc., with instructions for carrying out the activity directed from a central location.

To motivate the methodological developments that follow, consider the open-source Enron email corpus, which was made public during the federal investigation of the Enron scandal[3]. This dataset, along with a thorough explanation of its origin, is available at `http://www-2.cs.cmu.edu/~enron/`. In this paper, we consider the daily Enron email networks observed between January 1, 2001 through December 2, 2001, resulting in a time series of 240 consecutive days of *directed* email communications. However, we removed the outlier digraphs corresponding to Independence Day (July 4), Labor Day (Sept 3), and the day of the Sept 11 terrorist attacks, resulting in a total of 237 days.

Suppose the first 100 days are representative of the in-control communication flows at Enron, i.e., communications that are consistent with normal operations. Then Figure 5 shows the time series of daily *proportions* of mutual dyads and transitive triads over the first 100 days. Note that we use proportions of mutual dyads and transitive triads instead of counts as the size of the network is not constant over time. Notice that both processes appear to be stable over the first 100 days, although there looks to be evidence of autocorrelation. In addition, the average proportion of mutual dyads is 4.0×10^{-4}, while the average proportion of transitive triads is 6.5×10^{-7}, suggesting Enron's communication flows were generally sparse and asymmetric.

It is important to note that our goal is not to detect sustained shifts in the mean of the joint process. Instead, because in the limit of low reciprocity and high transitivity one obtains the fully transitive tournament, our interest then lies in detecting increases in the proportion of digraphs having a reciprocal tendency lower than expected *and* a transitive tendency higher than expected. To accomplish this, let μ_M and μ_T denote the in-control mean proportions of mutual dyads and transitive triads, respectively. Define the indicator random variable at time i as $Y_i = I_A = 1$ if the event A occurs and zero otherwise. Then let $A \equiv (X_{iM} < \mu_M) \cap (X_{iT} > \mu_T)$, where X_{iM} and X_{iT} denote the observed proportions of mutual dyads and transitive triads for the i^{th} digraph, respectively. So if the event A occurs at time i, then $Y_i = 1$ and the i^{th} digraph is classified as hierarchical. Figure 6

[3] `https://en.wikipedia.org/wiki/Enron_scandal`

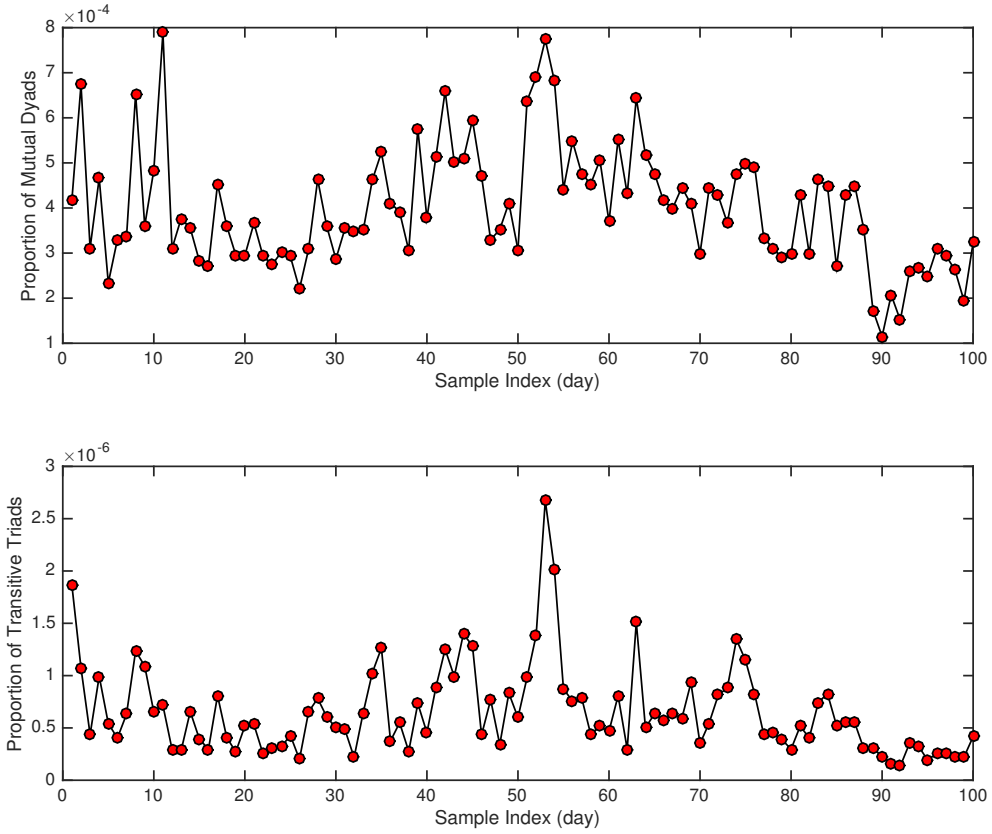

Figure 5: Time series of proportion of mutual dyads and proportion of transitive triads over the first 100 days of 2001 calendar year.

shows a scatterplot of the proportions of mutual dyads versus transitive triads for the in-control Enron networks. Notice that only 5 of the 100 observed digraphs are contained in the upper left quadrant, and thus, are classified as hierarchical. This result is not surprising as it is well known that Enron's organizational structure was radically decentralized, e.g., see Seeger and Ulmer (2003).

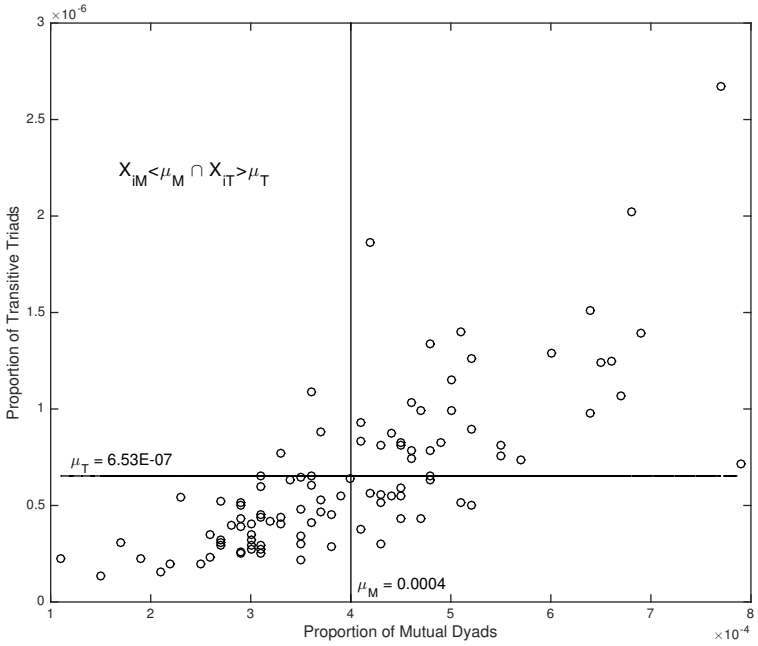

Figure 6: Scatterplot of proportion of mutual dyads versus proportion of transitive triads over first 100 days of the daily Enron email networks.

Now consider the scatterplot shown in Figure 7, where all 237 data points were plotted. It should be clear that the frequency of digraphs contained in the upper left quadrant increased significantly after the first 100 days. For example, over the first 100 days, the estimated probability of observing a hierarchical digraph was 0.05, or 5%. However, using the data obtained after the in-control period, i.e., days 101-237, this probability was estimated at approximately 0.18, or 18%, which is a 260% relative increase from the in-control probability. Clearly, the structure of Enron's email communication flows shifted to a more hierarchical or centralized tendency at some point following day 100. Such a large observed increase could in fact be due to the now well known crisis that was going on within Enron during that time. In retrospect, if Enron stakeholders had implemented a monitoring scheme to detect increases in the hierarchical tendencies of the communication flows, this could have potentially provided some early indication of the serious

internal problems Enron was facing.

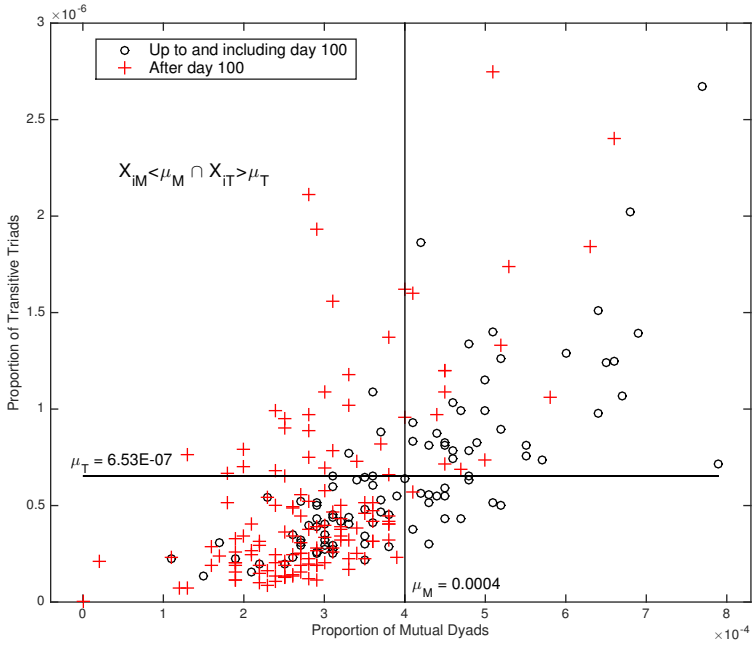

Figure 7: Scatterplot of proportion of mutual dyads versus proportion of transitive triads for all 237 daily Enron email networks. Note that the first 100 digraphs are assumed to be from the in-control process.

In this example, note that daily digraphs were classified as either hierarchical with probability p or not hierarchical with probability $1 - p$, so that Y was a Bernoulli random variable. In general, one can consider classifying the observed digraph at time i into one of k classes. For example, suppose we want to classify digraphs into one of the four quadrants shown in Figure 7, in which case we have a multinomial process with $k = 4$. Thus, the general problem considered in this paper is one of detecting change points in a k-class multinomial process with $n = 1$. Although the idea of applying SPC methods to monitor network systems is new, the general problem of monitoring multinomial processes has been studied. An extensive review of control charts for multinomial and multiattribute data is given in Topalidou and Psarakis (2009); however, in what follows we outline those developments that are most relevant to our general problem.

The SPC literature on monitoring multinomial processes is mostly concerned with the special case of $k = 2$, or the binomial process. The Shewhart p-chart is the traditional approach to monitoring binomial processes, but is not useful when $n = 1$. Cumulative sum (CUSUM) control charts are applicable, and are easily

constructed for the Bernoulli process, e.g., see Reynolds and Stoumbos (1999). For multinomial processes, Marcucci (1985) proposed a generalized p-chart to account for $k > 2$ using Pearson's chi-square statistic. However, as with the $k = 2$ case, this chart is not useful when $n = 1$. Ryan et al. (2011) proposed a multinomial CUSUM control chart derived from the sequential probability ratio test under a multinomial model with $n = 1$, while Weiβ (2012) proposed two control charting strategies using "comparative statistics" and a w-size moving average estimator of the class probabilities. Yashchin (2012) discussed multinomial control charting strategies using generalized likelihood ratio tests.

Given that the EWMA control chart is one of the most popular tools in today's SPC practice, it is surprising to find the literature lacking in EWMA control charting strategies for multinomial processes. One exception is Gan (1990), who proposed a modified EWMA control chart for use with binomial data. Steiner (1998) proposed a grouped-data EWMA control chart for continuous data distributions. It is important to note that our problem assumes a k-class multinomial process, while Steiner's problem assumes an underlying continuous process with observations classified into one of k groups. Thus, Steiner's method could perhaps be applicable to our problem if we were only interested in monitoring for shifts in the mean of one of the marginal variables, i.e., mutuality or transitivity, and we could only observe enough information on the variables to classify observations into one of the k groups. Unfortunately, this is not the problem being addressed in this paper.

Historically, the EWMA control charting strategy has been an attractive tool for the SPC practitioner. They are simple to design and implement, and are known to have detection properties similar to that of the CUSUM control chart. Further, upon signaling, the EWMA control chart offers reliable estimates of the process change point and magnitude of change. Due to wide acceptance of the EWMA in SPC practice, we propose a new EWMA control charting strategy for the general multinomial process. In addition to the monitoring of interpersonal organizational networks, our proposed EWMA control chart can find application across many other areas as well, including manufacturing and health care applications.

The remainder of this paper is organized as follows. In the next section, we propose a simple EWMA control charting strategy for multinomial processes that can be used to quickly detect changes in the probabilities of the k classes. Subsequently, we evaluate the detection performance of our new control chart for the $k = 2$ case relative to CUSUM strategy discussed in Reynolds and Stoumbos (1999). For the $k > 2$, we evaluate detection performance relative to the multinomial CUSUM strategy discussed in Ryan et al. (2011). We then apply our new charting strategy to the Enron email data to illustrate its application in practice. Finally, we close with a summary and discussion section.

2 Proposed EWMA Monitoring Strategy

Let $\mathbf{Y} \sim \text{multinomial}(n, \mathbf{p})$, where n denotes the number of independent trials, $\mathbf{Y}$ is a $k-$dimensional random vector of class counts such that $\sum_{j=1}^{k} Y_j = n$ and $\mathbf{p}$ is a $k-$dimensional vector of class probabilities such that $\sum_{j=1}^{k} p_j = 1$. Let us consider the linear combination of the class counts given by

$$Z = \sum_{j=1}^{k} w_j Y_j \tag{1}$$

where w_j is a weight applied to the j^{th} category. Then the expected value and variance of Z are easily shown to be

$$\mu_Z = n \sum_{j=1}^{k} w_j p_j \tag{2}$$

and

$$\sigma_Z^2 = n \left(\sum_{j=1}^{k} w_j^2 p_j (1 - p_j) - 2 \sum_{j=1}^{k-1} \sum_{j'=j+1}^{k} w_j w_{j'} p_j p_{j'} \right), \tag{3}$$

respectively.

Denote the in-control vector of multinomial class probabilities by $\mathbf{p}_0$, and the out-of-control vector by $\mathbf{p}_1$, where $\mathbf{p}_1 \neq \mathbf{p}_0$. In this paper, we define the weight for the j^{th} class by $w_j = (np_{0j})^{-1}$, or the inverse of class j's expected count. Then, if the process is in-control

$$\mu_{Z|\mathbf{p}=\mathbf{p}_0} = k \tag{4}$$

and

$$\sigma^2_{Z|\mathbf{p}=\mathbf{p}_0} = \frac{1}{n} \left(\sum_{j=1}^{k} \frac{1 - p_{0j}}{p_{0j}} - k(k-1) \right), \tag{5}$$

where, if the process is out-of-control

$$\mu_{Z|\mathbf{p}=\mathbf{p}_1} = \sum_{j=1}^{k} \frac{p_{1j}}{p_{0j}}$$

and

$$\sigma^2_{Z|\mathbf{p}=\mathbf{p}_1} = \frac{1}{n} \left(\sum_{j=1}^{k} \frac{p_{1j}(1 - p_{1j})}{p_{0j}^2} - 2 \sum_{j=1}^{k-1} \sum_{j'=j+1}^{k} \frac{p_{1j} p_{1j'}}{p_{0j} p_{0j'}} \right).$$

Note that if $p_{0j} = 1/k$ for all $j = 1, ..., k$, then $\sigma_Z^2 = 0$, regardless of whether or

not the process is in-control. Thus, the variance of Z is minimized at zero when the in-control multinomial cell probabilities are all equal, i.e., Z is not a random variable in this case. Consequently, the methodology developed in this section should not be applied in cases where the in-control class probabilities are equal.

At this point our goal is to set up an EWMA control chart on the random variable Z. To this end, let $\mathbf{Y}_i$ denote the vector of multinomial cell counts observed at time i ($i = 1, ..., N$), so that $Z_i = \sum_{j=1}^{k} w_j Y_{ij}$ denotes the linear combination of the cell counts at time i. Then, define the standardized linear combination at time i by

$$U_i = \frac{Z_i - \mu_{Z|\mathbf{p}=\mathbf{p}_0}}{\sigma_{Z|\mathbf{p}=\mathbf{p}_0}},$$

where $E(U_i) = 0$ and $Var(U_i) = 1$ *if the process is in-control*. One can chart an EWMA of U, or

$$G_i = rU_i + (1 - r)G_{i-1}, \tag{6}$$

and with each new sample compare to the upper and lower control limits given by

$$LCL_i/UCL_i = \pm L\sqrt{\frac{r}{2 - r}[1 - (1 - r)^{2i}]}, \tag{7}$$

where $0 < r < 1$, $G_0 = 0$ and L is a constant chosen by the practitioner to achieve an acceptable in-control average run length, or ARL. Recall that the ARL is the average number of runs before the control chart signals. Note that the control limits in Equation (7) are the transient limits; however, often times it is more convenient to use the steady-state control limits given by

$$LCL_1/UCL_1 = \pm L\sqrt{\frac{r}{2 - r}}. \tag{8}$$

For the general multinomial process, one can estimate the ARLs of the proposed EWMA control chart using Monte Carlo simulation[4]. However, for the special-case of $n = 1$, a slightly modified version of the Markov chain model proposed by Borror et al. (1998) can provide good analytical approximations. Specifically, let the in-control region in Equation (8) be divided up into s subintervals or states, where state $s + 1$ is absorbing and represents the out-of-control region both above and below the control limits. Then, the transition probability, $P(t, t')$, is the probability of moving from state t to state t' in one step and is given by

$$P(t, t') = P[U < B(t, t')] - P[U < A(t, t')] \tag{9}$$

[4]A C++ implementation of a Monte Carlo simulation model of the proposed EWMA control chart is available from the first author upon request.

where

$$A(t,t') = LCL_1 + \left(\frac{UCL_1 - LCL_1}{2sr}\right)[2(t'-1) - (1-r)(2t-1)]$$

and

$$B(t,t') = LCL_1 + \left(\frac{UCL_1 - LCL_1}{2sr}\right)[2t' - (1-r)(2t-1)]$$

with probabilities on U easily obtained from

$$P(Y_j = 1) = P(Z = w_j) = P\left(U = \frac{w_j - \mu_{Z|\mathbf{p}=\mathbf{p}_0}}{\sigma_{Z|\mathbf{p}=\mathbf{p}_0}}\right) = P(U = u_j) = p_j$$

for $j = 1, 2, ..., k$. Let $\mathbf{Q}$ denote the $s \times s$ matrix obtained from the transition probability matrix $\mathbf{P}$ by deleting the row and column associated with the absorbing state, then Brook and Evans (1972) showed that the $s \times 1$ ARL vector $\mathbf{R}$ is the solution to the system $(\mathbf{I} - \mathbf{Q})\mathbf{R} = \mathbf{1}$, where $\mathbf{I}$ is the $s \times s$ identity matrix and $\mathbf{1}$ is a $s \times 1$ vector of ones. Hence, $\mathbf{R} = (\mathbf{I} - \mathbf{Q})^{-1}\mathbf{1}$ is simply the ARLs, given the control chart started in the various states. Thus, the ARL given $G_0 = 0$ is just the middle, or the $\frac{(s+1)}{2}^{th}$, element of $\mathbf{R}$.

Note that the ARLs given in the vector $\mathbf{R}$ are initial-state ARLs, i.e., elements of the $s \times 1$ vector $\mathbf{R}$ consist of ARL approximations given that the process is out-of-control from the very beginning. Instead, one might be interested in the steady-state ARLs, i.e., ARLs given that the process is in-control for some time, then shifts out-of-control. One can easily obtain approximations to the steady-state ARLs using the Markov chain model described above. Specifically, let the matrix $\mathbf{P}_0$ denote the transition probability matrix for the in-control process and $\mathbf{Q}_0$ the matrix obtained from $\mathbf{P}_0$ by deleting the row and column associated with the absorbing state. Then, add the probabilities in $\mathbf{P}_0$ associated with the absorbing state to the $\left(\frac{s+1}{2}\right)^{th}$ state of the matrix $\mathbf{Q}_0$, and call the resulting matrix $\tilde{\mathbf{Q}}_0$. This is justified on the basis that if the process is in control and a signal is issued, that signal is a false alarm. Once determined a false alarm, the statistics are reset and monitoring continues. Thus, the Markov chain is returned to the $\left(\frac{s+1}{2}\right)^{th}$ state.

By adding the probabilities associated with the absorbing state to the probabilities associated with the $\left(\frac{s+1}{2}\right)^{th}$ state we obtain a Markov chain with all positive recurrent states. The in-control stationary probability distribution $\boldsymbol{\pi}_0$ is then given by the dominant eigenvector of the matrix $\tilde{\mathbf{Q}}_0$. Although we do not know exactly which state the Markov chain will reside immediately preceding a process change, the stationary probability distribution $\boldsymbol{\pi}_0$ will give us the probabilities associated with the Markov chain being in any one state (prior to a process change). Thus, to obtain the steady state average run length, simply compute the weighted average

of R_t (i.e., the initial state ARL given the Markov chain started in state t) and the probability that the Markov chain is in state t prior to the process change, or $ARL_{Steady} = \boldsymbol{\pi}_0^{'}\mathbf{R}$.

To design the proposed EWMA control chart, the practitioner must specify the charting parameters r and L. In practice, r is typically chosen between 0.05 and 0.20, e.g., see Hawkins and Wu (2014), where smaller/larger values of r often result in a control chart that is more sensitive to smaller/larger changes in the parameter(s) being monitored. Once r is chosen, the Markov chain model discussed above can be used to select a value for L, given an acceptable *in-control* ARL, or ARL_0. For example, Figure 8 shows in-control ARL approximations for the proposed EWMA control chart applied to a Bernoulli process with in-control "success" probability $p_0 \in [0.05, 0.20]$ computed using the Markov chain with $s = 501$ states. Then, for such Bernoulli processes, one could use Figure 8 to help design the proposed control chart. To illustrate, reconsider the Enron email networks discussed earlier where the in-control proportion of hierarchical digraphs was $p_0 = 0.05$. Then from Figure 8 we find that if $L = 3$ we will obtain an in-control ARL of approximately 570. Both R and MATLAB implementations of the Markov chain model discussed above are available from the first author upon request.

In the next section we use Monte Carlo simulation to evaluate the out-of-control ARL performances of the proposed EWMA control chart, relative to CUSUM strategies. Subsequently, we demonstrate application of our proposed EWMA control chart using the open source Enron email corpus.

3 Average Run Length Performance

In this section we study the ARL performance of our proposed EWMA control chart. For the $k = 2$ case, we compare ARL performance between the EWMA chart, and the CUSUM control chart discussed in Gan (1993) and Reynolds and Stoumbos (1999). For the $k > 2$ case, we compare our results to those obtained from the multinomial CUSUM control chart published in Ryan et al. (2011). Because it is inefficient to artificially group items into samples of size n when observations are available successively on individual items, we only consider the $n = 1$ case. We should note that the EWMA control limits given in Equation (7) were used in our evaluations. Additionally, because most processes are likely to operate in-control for some period of time, and then shift out-of-control, we evaluated the steady-state ARLs for the out-of-control cases. Thus, in our simulation model, we assumed a change point following the 100^{th} sample, where if a control chart signaled on or before the change point, then the charting statistics were reset and monitoring continued.

To efficiently summarize ARL performance across the settings of the out-of-

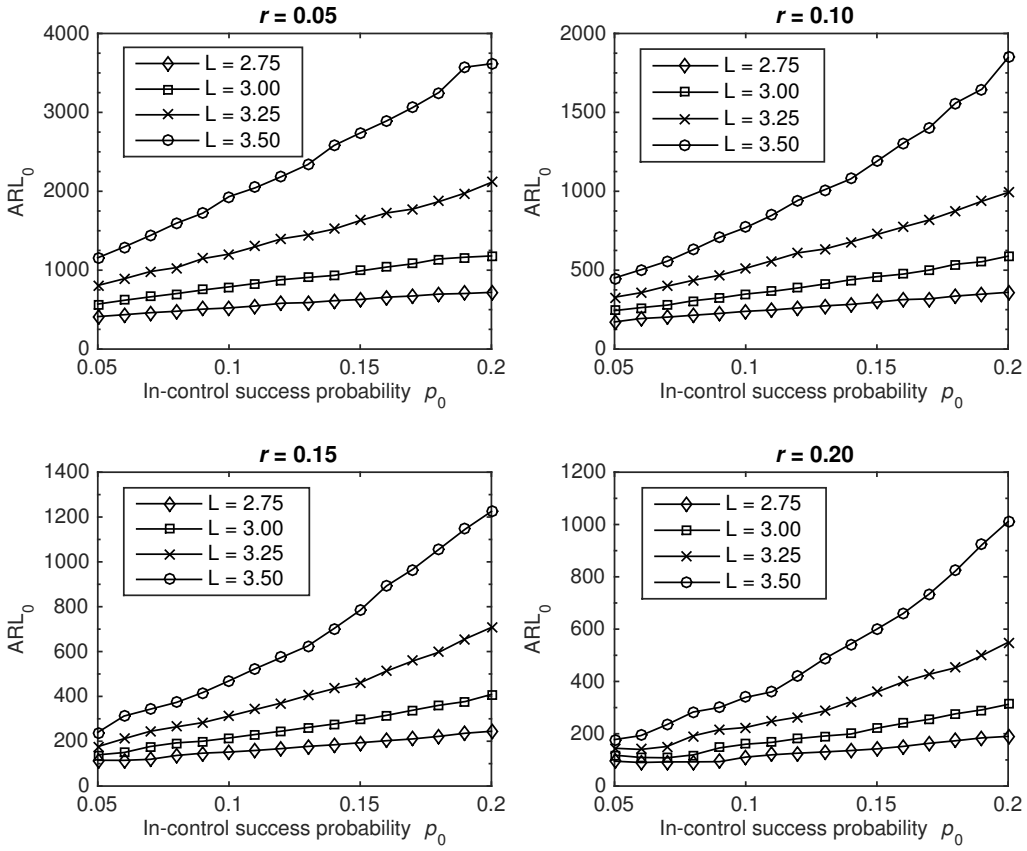

Figure 8: In-control ARL approximations for the proposed EWMA control chart applied to a Bernoulli process with $p_0 \in [0.05, 0.20]$. Markov chain model with $s = 501$ was used to calculate the ARLs.

control parameter values considered, we follow Han and Tsung (2004) and compute the relative mean index, or RMI, given by

$$RMI(\nu) = \frac{1}{m}\sum_{\ell=1}^{m}(ARL_{\mathbf{p}_{1\ell}}(\nu) - ARL^{*}_{\mathbf{p}_{1\ell}})(ARL^{*}_{\mathbf{p}_{1\ell}})^{-1},$$

where $ARL_{\mathbf{p}_{1\ell}}(\nu)$ is the ARL of control chart ν at the ℓ^{th} setting of $\mathbf{p}_1$, m is the total number of out-of-control settings of $\mathbf{p}_1$ being studied, and $ARL^{*}_{\mathbf{p}_{1\ell}}$ is the smallest ARL across all control charts being compared for the ℓ^{th} setting of $\mathbf{p}_1$. The control charting strategy with the best relative detection performance across the range of out-of-control parameter settings considered will then have the smallest RMI.

We first consider the Bernoulli process with two different values for the in-control probability, or $p_0 = 0.05$ and 0.10. For each case, we designed two different EWMA charts, i.e., $r = 0.05$ and $r = 0.10$ with $\text{ARL}_0 \approx 500$, and compared out-of-control steady-state ARL performance to that of two different Bernoulli CUSUM charts, i.e., one CUSUM chart designed for smaller changes in p, and the other designed for larger changes. The level of p for which a CUSUM chart was designed to quickly detect is denoted by p^*. The ARLs for all charts were obtained over 1 million independent Monte Carlo simulation runs. Table 1 shows ARL results for $p_0 = 0.05$, while Table 2 shows ARL results for $p_0 = 0.10$.

Tables 1 and 2 suggest that the Bernoulli CUSUM chart has the best detection performance at the setting of the out-of-control parameter p_1 for which it was designed to detect, or p^*. This is an expected result as it is well known that the CUSUM has theoretical optimality properties, e.g., see Moustakides (1986). Also, as expected, the EWMA chart is more sensitive to smaller shifts in p for smaller values of r, and vice versa. Note further that the EWMA chart can be designed to be competitive with the Bernoulli CUSUM, often yielding ARLs with little practical difference. In order to efficiently summarize relative ARL performance of the control charts across the range of p_1 investigated, Tables 1 and 2 also report the RMI for each control chart considered. Note that in both tables, the EWMA with $r = 0.10$ yields the smallest RMI measure amongst the control charts being compared, and thus, achieved the best relative detection performance when considering the entire range of p_1. These results suggest that, if the value of p^* cannot be specified *a priori*, then one might consider using the proposed EWMA chart as an alternative to the CUSUM strategy.

We now focus our attention to the $k > 2$ case, where we evaluate the proposed EWMA chart relative to the multinomial CUSUM chart proposed in Ryan et al. (2011). To help guide our study, we adopt the Case 1 and Case 4 scenarios given in Ryan et al. (2011). As before, we consider two different EWMA designs, i.e.,

Table 1: ARL comparisons between Bernoulli CUSUM and the proposed EWMA for a Bernoulli process with in-control success probability $p_0 = 0.05$. All control charts were calibrated to have in-control initial-state ARL of approximately 500.

	CUSUM	CUSUM	EWMA	EWMA
	$p^* = 0.10$	$p^* = 0.30$	$r = 0.05$	$r = 0.10$
p_1	$h = 2.95$	$h = 1.816$	$L = 2.999$	$L = 3.64$
0.10	66.68	88.04	76.99	85.57
0.15	30.86	36.38	33.36	35.73
0.20	19.78	21.17	20.56	21.05
0.25	14.58	14.53	14.76	14.59
0.30	11.56	10.98	11.48	11.07
0.35	9.60	8.81	9.40	8.92
0.40	8.23	7.39	7.96	7.45
0.45	7.20	6.37	6.90	6.41
0.50	6.42	5.61	6.10	5.62
0.60	5.28	4.56	4.94	4.51
0.70	4.48	3.86	4.16	3.78
0.80	3.90	3.35	3.59	3.27
0.90	3.45	2.96	3.15	2.87
$RMI =$	0.0988	0.0506	0.0801	0.0420

$r = 0.05$ and 0.10 with $\text{ARL}_0 \approx 500$. The first scenario, Case 1, involves $k = 3$ classes. Table 3 shows the ARL results, where the first row corresponds to the in-control setting. Note that the parameter values for which the CUSUM was designed to detect are shown in bold. From Table 3 it is clear that the multinomial CUSUM discussed in Ryan et al. (2011) performs relatively best. This result is not surprising, particularly because the direction of the shift in $\mathbf{p}$ is the same as that for which the CUSUM was designed. However, Table 4 shows that if the direction of the shift in $\mathbf{p}$ is misspecified, the relative performance of the CUSUM chart can suffer considerably.

Table 5 shows ARL results for Case 4 in Ryan et al. (2011). Notice that as the number of classes k gets larger, and if the shift in $\mathbf{p}$ is in the direction for which the CUSUM was designed, the multinomial CUSUM achieves even greater relative performance. Because the CUSUM is derived from a sequential probability ratio test, it is no surprise that it performs relatively better in this case. Table 6 shows ARL results for Case 4, but with the actual shift in $\mathbf{p}$ in a different direction than what the CUSUM was designed to detect. As in Case 1, notice that the relative performance of the CUSUM chart suffers greatly when the direction of the shift is

Table 2: ARL comparisons between Bernoulli CUSUM and the proposed EWMA for a Bernoulli process with in-control success probability $p_0 = 0.10$. All control charts were calibrated to have in-control initial-state ARL of approximately 500.

	CUSUM	CUSUM	EWMA	EWMA
	$p^* = 0.15$	$p^* = 0.35$	$r = 0.05$	$r = 0.10$
p_1	$h = 4.288$	$h = 2.40$	$L = 2.808$	$L = 3.26$
0.15	88.24	119.45	109.45	119.12
0.20	41.21	50.73	46.86	50.71
0.25	26.33	28.76	27.99	29.05
0.30	19.33	19.26	19.64	19.62
0.35	15.28	14.32	15.01	14.56
0.40	12.63	11.33	12.15	11.51
0.45	10.78	9.37	10.19	9.48
0.50	9.40	8.00	8.77	8.05
0.60	7.48	6.20	6.86	6.19
0.70	6.22	5.10	5.63	5.02
0.80	5.82	4.36	4.79	4.22
0.90	4.59	3.82	4.16	3.65
0.95	4.28	3.60	3.91	3.42
$RMI =$	0.1420	0.0636	0.1086	0.0580

misspecified.

General results in this section suggest that the proposed EWMA control chart is a viable alternative to the CUSUM chart. Although the CUSUM chart can be designed to perform best at a specific setting of the out-of-control parameter vector $\mathbf{p}_1$, in practice such a setting is often unknown. We showed via Monte Carlo simulation that, for Bernoulli processes, the proposed EWMA control chart with $r \in [0.05, 0.10]$ can often provide better relative performance than the Bernoulli CUSUM chart when the entire range of settings for p_1 is considered. Results also suggest that as the number of classes k increases, the relative performance of the CUSUM chart increases when the true shift direction is specified correctly. However, when the shift direction is misspecified, the relative performance of the CUSUM chart suffers considerably. Therefore, in cases where the shift in $\mathbf{p}$ cannot be specified with certainty, the proposed EWMA control chart should be considered as an alternative.

Table 3: ARL comparisons between proposed EWMA and the multinomial CUSUM published in Ryan et al. (2011) for Case 1. First row corresponds to the in-control case. Parameter values for which the CUSUM was designed are shown in bold.

			Multinomial	EWMA	EWMA
p_1	p_2	p_3	CUSUM	$r = 0.05$	$r = 0.10$
P(Good)	P(Fair)	P(Bad)	$h = 3.47$	$L = 2.702$	3.081
0.65	*0.25*	*0.10*	508.31	508.31	508.43
0.625	0.255	0.12	236.73	247.72	250.18
0.6	0.26	0.14	132.43	132.36	141.94
0.55	0.27	0.18	57.28	57.26	62.32
0.5	0.28	0.22	32.68	33.72	35.52
0.4517	**0.2999**	**0.2484**	23.44	24.96	25.64
0.35	0.35	0.30	14.69	16.45	16.10
0.25	0.4	0.35	10.65	12.25	11.60
0.15	0.45	0.40	8.34	9.77	9.01
0.05	0.5	0.45	6.85	8.13	7.33
		$RMI=$	~ 0.0000	0.0857	0.0815

4 Application to Enron Email Corpus

In this section we apply our new EWMA control chart to the Enron email corpus discussed earlier in efforts to detect if and when an increase in the hierarchical tendency of the organization's communication structure occurred. Recall for this data set $k = 2$ and $\mathbf{p}_0 = [0.05, 0.95]$, so that the linear combination of the class counts at time i is given by

$$z_i = 0.05^{-1} y_i + 0.95^{-1}(1 - y_i)$$

where y_i is the observed value of the Bernoulli random variable at time i, i.e., $y_i = 1$ if digraph i was classified as hierarchical and zero otherwise. The mean and standard deviation of Z, given the process is in-control, are computed from Equations (4) and (5), respectively, and are given by $\mu_Z = 2$ and $\sigma_Z \approx 4.13$, so that we compute the standardized linear combination at time i by

$$u_i = \frac{z_i - 2}{4.13}.$$

Table 4: ARL comparisons between proposed EWMA and the multinomial CUSUM published in Ryan et al. (2011) for misspecified Case 1. First row corresponds to the in-control case.

			Multinomial	EWMA	EWMA
			CUSUM	$r = 0.05$	$r = 0.10$
p_1	p_2	p_3	$h = 3.47$	$L = 2.702$	$L = 3.081$
0.65	*0.25*	*0.10*	508.31	508.31	508.43
0.66	0.22	0.12	315.95	316.06	299.56
0.67	0.20	0.13	271.98	255.29	243.73
0.68	0.18	0.14	237.18	211.15	202.97
0.69	0.15	0.16	174.90	144.73	141.03
0.72	0.10	0.18	151.97	116.59	112.56
0.73	0.07	0.20	120.17	89.07	86.45
0.74	0.05	0.21	111.28	80.63	78.13
0.75	0.02	0.23	91.77	65.24	63.03
		$RMI=$	0.2750	0.0378	0.0000

Using $r = 0.10$, the EWMA statistic $G_i = 0.10u_i + 0.90G_{i-1}$ for $i = 1, 2, ..., 237$ was plotted and compared to the upper control limit given in Equation (7) with $L = 3.64$. This value of L corresponds to an in-control ARL of approximately 500. Figure 9 shows the control chart, where the first signal occurred with digraph 119, corresponding to June 16, 2001.

If we take a retrospective look at Enron's process, we see a very large increase in the hierarchical tendency of the interpersonal communications from approximately mid-June to mid-September. Note that the proposed control chart detected the onset of the shift very quickly. To obtain an estimate for the change point, we can use the "built-in" change point estimator of the EWMA chart, e.g., see Nishina (1992) and Perry and Pignatiello (2011). Specifically, let τ denote the true change point, i.e., the last sample obtained from the unchanged process, then the estimate using the EWMA control chart is given by $\hat{\tau} = \max[i : G_i \leq 0]$, i.e., the most recent time period where the EWMA statistic is less than or equal to zero. For the Enron process, the change point is then estimated at $\hat{\tau} = 115$, suggesting the first digraph from the out-of-control process is that sampled on day 116, or June 11, 2001. To obtain an estimate for the out-of-control p_1, we can compute the average of the y_i's from samples $i = \hat{\tau} + 1, ..., T$, where T denotes the time of control chart signal. Thus, with $T = 119$ we obtain $\hat{p}_1 = 1/2$, and we find an estimated relative percent increase of 900% from the in-control value.

As mentioned earlier, it is well known that Enron's organizational structure

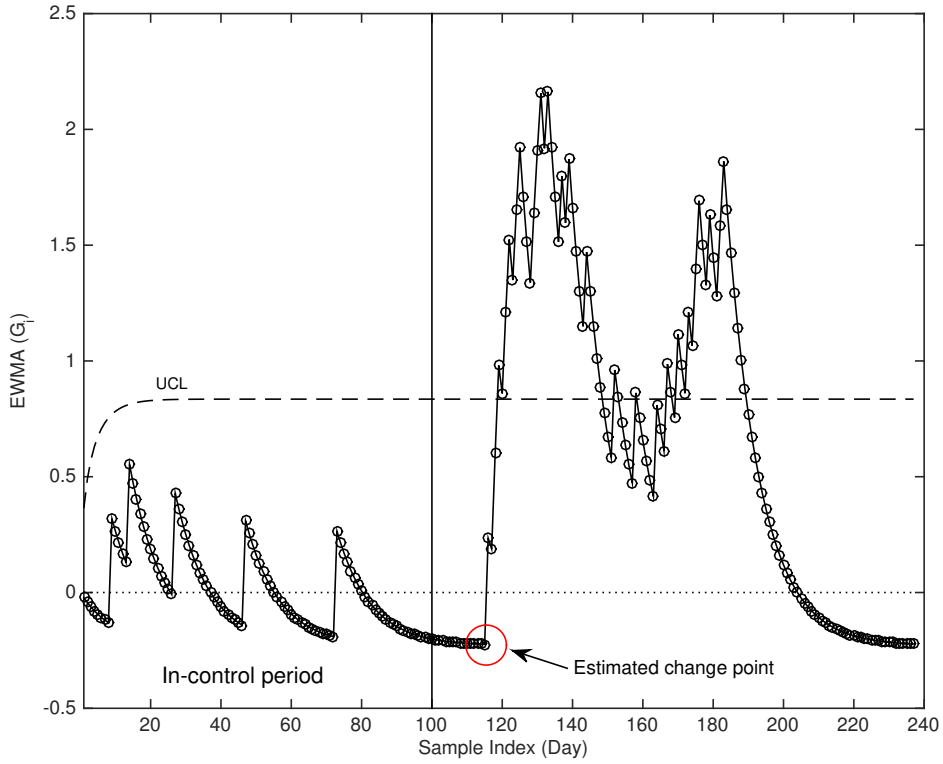

Figure 9: Proposed EWMA control chart applied to Enron email networks with $p_0 = 0.05$, $r = 0.10$ and $L = 3.64$. In-control ARL is approximately 500. Control chart signaled on day 119, or June 14, 2001. Large shift observed from mid-June to mid-September.

Table 5: ARL comparisons between proposed EWMA and multinomial CUSUM published in Ryan et al. (2011) for Case 4. First row corresponds to the in-control case. Parameter values for which the CUSUM was designed are shown in bold.

				Multinomial CUSUM	EWMA $r = 0.05$	EWMA $r = 0.10$
p_1	p_2	p_3	p_4	$h = 3.7992$	$L = 2.721$	$L = 3.216$
0.65	*0.20*	*0.10*	*0.05*	499.62	500.20	499.47
0.60	0.22	0.12	0.06	179.87	207.16	239.25
0.55	0.24	0.14	0.07	83.72	104.05	128.34
0.50	0.26	0.16	0.08	46.93	62.78	78.30
0.46	0.28	0.17	0.09	32.70	45.86	55.94
0.396	**0.3283**	**0.1734**	**0.1023**	21.31	33.73	39.94
0.35	0.34	0.19	0.12	16.59	25.01	28.31
0.30	0.35	0.21	0.14	13.27	19.27	20.86
0.25	0.36	0.23	0.16	11.04	15.61	16.36
0.20	0.38	0.24	0.18	9.46	13.30	13.57
0.15	0.40	0.25	0.20	8.27	11.61	11.59
0.10	0.42	0.26	0.22	7.34	10.28	10.10
0.05	0.43	0.28	0.24	6.59	9.13	8.87
			$RMI=$	0.0000	0.3905	0.5361

was very decentralized. Thus, such a large increase in the probability of observing a hierarchical digraph is alarming, and may suggest mid-June was the beginning of the end of Enron. It is interesting to note that around the time of the estimated change point, two significant events did occur. First, Enron closed down the controversial Dabhol Power Plant (DPP) in Maharashtra, India, due to a payment and contract dispute between the local state government and the plant owners (Enron owned 65% of DPP). Enron claimed to have incurred over $1 billion in losses for the plant. Second, the Federal Energy Regulatory Commission (FERC) instituted price caps across the western United States, putting an end to the California energy crisis[5]. This was problematic for Enron as much of the cash flows keeping Enron afloat were from manipulating the energy markets in the west, and these new price caps prevented this from happening. Although we cannot state with certainty that the aforementioned events *caused* the control chart signal, it is possible that these events contributed significantly to the ultimate demise of Enron on December 2, 2001.

[5] `https://en.wikipedia.org/wiki/California_electricity_crisis`

Table 6: ARL comparisons between proposed EWMA and multinomial CUSUM published in Ryan et al. (2011) for misspecified Case 4. First row corresponds to the in-control case.

				Multinomial CUSUM	EWMA $r = 0.05$	EWMA $r = 0.10$
p_1	p_2	p_3	p_4	$h = 3.7992$	$L = 2.721$	$L = 3.216$
0.65	*0.20*	*0.10*	*0.05*	499.62	500.20	499.47
0.625	0.15	0.15	0.075	238.35	113.77	131.91
0.60	0.10	0.20	0.10	133.49	49.36	56.70
0.55	0.05	0.25	0.15	58.70	23.02	24.34
0.50	0.025	0.30	0.175	35.00	16.71	17.05
0.45	0.02	0.35	0.18	24.49	14.23	14.40
0.40	0.015	0.40	0.185	18.43	12.38	12.37
0.35	0.01	0.45	0.19	14.66	10.93	10.81
0.30	0.005	0.50	0.195	12.10	9.77	9.57
0.25	0.0025	0.55	0.1975	10.29	8.90	8.64
0.20	0.001	0.60	0.199	8.95	8.18	7.89
			$RMI=$	0.7601	0.0101	0.0397

5 Concluding Remarks

Increases in the hierarchical tendency of an organization's interpersonal communications network might suggest a shift to a more hierarchical decision-making structure, where all decisions and processes are handled at the top of the organization. Unfortunately, such a structure can often lead to slower decision making, decreased operational efficiency, and less innovation. Further, the literature on organizational research suggests the root cause of such an increase could be associated with conflict or crisis within the organization. In this paper we considered the important problem of detecting shifts in the hierarchical tendency of interpersonal networks over time, as the early detection of increases can potentially reveal the onset of conflict or crisis within the organization. As a result, organizational managers can implement a crisis or conflict management plan sooner so that the effects of the crisis on the health of the organization are minimized.

To this end, we demonstrated that our network monitoring problem can be reduced to that of monitoring a Bernoulli process, where digraphs having lower than expected reciprocal ties *and* higher than expected transitive ties are classified as hierarchical, otherwise they are classified as non-hierarchical. This is justified by the fact that in the limit of low reciprocity and high transitivity one obtains

the fully transitive tournament. We then proposed an EWMA control charting strategy for the general multinomial process, where the Bernoulli process is an important special case. For $n = 1$, we discussed a Markov chain representation of the proposed EWMA control chart that can be used to assess the average run length properties in practice.

Monte Carlo simulation was used to study the out-of-control ARL performance of the proposed EWMA control chart, relative to CUSUM strategies. Our general results suggest that the proposed EWMA chart is a viable alternative to the CUSUM strategies when the magnitude and/or the direction of the actual shift is different than what the CUSUM chart was designed to detect. Thus, when the practitioner cannot specify the magnitude and/or direction of the shift in $\mathbf{p}$ *a priori*, we recommend use of the proposed EWMA control chart.

To demonstrate how the proposed control chart is applied in practice, we considered the daily Enron email networks observed during the year 2001, or Enron's crisis year. Through our analysis it was estimated that a significant increase in the hierarchical tendency of the email communications network at Enron occurred at or around June 11, 2001, approximately 6 months before the organization filed for bankruptcy. Assuming the observed increase was a result of the ongoing crisis within the Enron organization during that time, then the proposed control chart was able to detect the onset of this crisis rather quickly.

Finally, in addition to the network monitoring application discussed in this paper, the proposed EWMA control chart is applicable to a wide range of other applications. For example, the proposed strategy is generally applicable to multinomial processes, which are prevalent in both the manufacturing and healthcare industries.

References

Borror, C. M., C. W. Champ, and S. E. Rigdon (1998). Poisson EWMA control charts. *Journal of Quality Technology 30*(4), 352–361.

Brook, D. and D. A. Evans (1972). An approach to the probability distribution of CUSUM run length. *Biometrika 59*(3), 539–549.

Contractor, N. S., S. Wasserman, and K. Faust (2006). Testing multitheoretical, multilevel hypotheses about organizational networks: An analytical framework and empirical example. *Academy of Management Review 31*(3), 681–703.

Cropanzano, R. and M. S. Mitchell (2005). Social exchange theory: An interdisciplinary review. *Journal of Management 31*(6), 874–900.

Danowski, J. A. and P. Edison-Swift (1985). Crisis effects on intraorganizational computer-based communication. *Communication Research 12*(2), 251–270.

Davis, J., L. Hossain, and S. H. Murshed (2007). Social network analysis and organizational disintegration: The case of Enron corporation. In *ICIS Proceedings*. Association for Information Systems.

Diesner, J., T. Frantz, and K. Carley (2005). Communication networks from the Enron email corpus: "it's always about the people. Enron is no different". *Computational and Mathematical Organization Theory 11*, 201–228.

Gan, F. F. (1990). Monitoring observations generated from a binomial distribution using modified exponentially weighted moving average control chart. *Journal of Statistical Computation and Simulation 37*, 45–60.

Gan, F. F. (1993). An optimal design of CUSUM control charts for binomial counts. *Journal of Applied Statistics 20*, 445–460.

Han, D. and F. Tsung (2004). A generalized EWMA control chart and its comparison with the optimal EWMA, CUSUM, and GLR schemes. *The Annals of Statistics 32*, 316–339.

Hawkins, D. M. and Q. Wu (2014). The CUSUM and the EWMA head-to-head. *Quality Engineering 26*(2), 215–222.

Heider, F. (1958). *The Psychology of Interpersonal Relations*. John Wiley.

Hillman, A. J., M. C. Withers, and B. J. Collins (2009). Resource dependence theory: A review. *Journal of Management 35*(6), 1404–1427.

Holland, P. and S. Leinhardt (1971). Transitivity in structural models of small groups. *Small Group Research 2*(2), 107–124.

Holland, P. and S. Leinhardt (1976). Local structure in social networks. *Sociological Methodology 7*, 1–45.

Kilduff, M. and W. Tsai (2003). *Social Networks and Organizations*. Sage.

Lin, D. K. J. (2014). Comments: Some challenges for multivariate statistical process control. *Quality Engineering 98*, 26–96.

Marcucci, M. (1985). Monitoring multinomial processes. *Journal of Quality Technology 17*(2), 86–91.

Moody, J. (1998). Matrix methods for calculating the triad census. *Social Networks 20*, 291–299.

Moustakides, G. (1986). Optimal stopping times for detecting changes in distributions. *The Annals of Statistics 14*(4), 1379–1387.

Nishina, K. (1992). A comparison of control charts from the viewpoint of change-point estimation. *Quality and Reliability Engineering International 8*(6), 537–541.

Perry, M. B. and J. J. Pignatiello (2011). Estimating the time of step change with poisson CUSUM and EWMA control charts. *International Journal of Production Research 49*(10), 2857–2871.

Reynolds, M. and Z. Stoumbos (1999). A CUSUM chart for monitoring a proportion when inspecting continuously. *Journal of Quality Technology 31*, 87–108.

Ryan, A. G., L. J. Wells, and W. H. Woodall (2011). Methods for monitoring multiple proportions when inspecting continuously. *Journal of Quality Technology 43*(3), 237–248.

Seeger, M. W. and R. R. Ulmer (2003). Explaining Enron: Communication and responsible leadership. *Management Communication Quarterly 17*(1), 58–84.

Steiner, S. H. (1998). Grouped data exponentially weighted moving average control charts. *Journal of the Royal Statistical Society, Series C 47*(2), 203–216.

Topalidou, E. and S. Psarakis (2009). Review of mulrinomial and multiattribute quality control charts. *Quality and Reliability Engineering International 25*(7), 773–804.

Weiβ, C. H. (2012). Continuously monitoring categorical processes. *Quality Technology and Quantitative Management 9*(2), 171–188.

Woodall, W. H., M. J. Zhao, K. Paynabar, R. Sparks, and J. D. Wilson (2017). An overview and perspective on social network monitoring. *IISE Transactions 49*, 354–365.

Yashchin, E. (2012). On detection of changes in categorical processes. *Quality Technology and Quantitative Management 9*(1), 79–96.